



**HAL**  
open science

## Characterization and modeling of the viscoelasticity of pharmaceutical tablets

Léo Desbois, Pierre Tchoreloff, Vincent Mazel

► **To cite this version:**

Léo Desbois, Pierre Tchoreloff, Vincent Mazel. Characterization and modeling of the viscoelasticity of pharmaceutical tablets. *International Journal of Pharmaceutics*, 2020, 587, pp.1-7. 10.1016/j.ijpharm.2020.119695 . hal-03166915

**HAL Id: hal-03166915**

**<https://hal.inrae.fr/hal-03166915>**

Submitted on 22 Aug 2022

**HAL** is a multi-disciplinary open access archive for the deposit and dissemination of scientific research documents, whether they are published or not. The documents may come from teaching and research institutions in France or abroad, or from public or private research centers.

L'archive ouverte pluridisciplinaire **HAL**, est destinée au dépôt et à la diffusion de documents scientifiques de niveau recherche, publiés ou non, émanant des établissements d'enseignement et de recherche français ou étrangers, des laboratoires publics ou privés.



Distributed under a Creative Commons Attribution - NonCommercial 4.0 International License

# 1                    **Characterization and modeling of the viscoelasticity of** 2                    **pharmaceutical tablets**

3                    Léo Desbois<sup>1</sup>, Pierre Tchoreloff<sup>1</sup>, Vincent Mazel<sup>1,\*</sup>

4                    <sup>1</sup>Univ. Bordeaux, CNRS, Arts et Metiers Institute of Technology, Bordeaux INP,  
5                    INRAE, I2M Bordeaux, F-33400 Talence, France

6                    \*corresponding author : Université de Bordeaux, I2M Bordeaux, 146 rue Léo Saignat,  
7                    F-33000 Bordeaux, France ; tel :+33 5 57 57 92 60 ; E-mail address:  
8                    vincent.mazel@u-bordeaux.fr

## 9                    **Abstract**

10                   Evolution of the compaction properties of powders with the compaction speed (strain  
11                   rate sensitivity, SRS) is a common phenomenon during the manufacturing of  
12                   pharmaceutical tablets. Nevertheless, several different phenomena can be  
13                   responsible of the SRS like friction, viscoelasticity, viscoplasticity or air entrapment. In  
14                   this work, an original experimental methodology was developed to characterize  
15                   specifically the viscoelasticity of tablets using a compaction simulator. After various  
16                   compressions, tablets were finally loaded elastically at different constant strain rates.  
17                   This methodology made it possible to measure the apparent bulk and shear moduli  
18                   as a function of the strain rate. The methodology was successfully applied to  
19                   microcrystalline cellulose (MCC), Starch, Lactose monohydrate (GLac) and  
20                   Anhydrous Calcium Phosphate (ACP). No significant evolution of the moduli was  
21                   found for Lac and ACP as expected. On the contrary, for MCC and Starch, both  
22                   shear and bulk moduli were found to increase along with the strain rate. The  
23                   viscoelastic behavior was then successfully modeled using prony series. Assessment

24 of the model parameters was achieved by inverse identification using an analytical  
25 model and a finite element analysis.

26 **keywords:** viscoelasticity, compaction, speed, strain rate sensitivity, mechanical  
27 behavior, tablet

## 28 **1. Introduction**

29 The tablet is the most popular solid dosage form in the pharmaceutical industry.  
30 Nevertheless, the mechanical phenomena occurring during the manufacturing  
31 process are complex and still not fully understood. Even if the compaction process is  
32 used for more than a century, some manufacturing problems are still challenging  
33 today, like, for example, capping or sticking.

34 Scale-up is a critical aspect during the development of new tablets, because some  
35 problems may remain undetected during development. Historically, for the  
36 development of tablets, companies used eccentric presses whereas final production  
37 was generally performed on rotary presses. However, tablets produced on an  
38 eccentric machine might differ from those produced on rotary presses especially  
39 because the kinematic of this two kinds of presses is very different. To fill the gap,  
40 compaction simulators were created to be able, at the development scale, to mimic  
41 the kinematic behavior of the industrial rotary presses.

42 In fact, on industrial rotary presses, compaction speed can be very high and it is well  
43 known that this speed can have consequences on the final tablet quality attributes.  
44 This phenomena is often called Strain Rate Sensitivity (SRS)(Armstrong, 1989).  
45 Several aspects can explain the SRS. The first one is air entrapment. When the  
46 compaction speed increases, air can have difficulties to escape from the tablet and  
47 this can imply a modification of the apparent deformation behavior of the powder

48 (Casahoursat et al., 1988; Garr and Rubinstein, 1991). In addition, defects can  
49 appear inside or at the surface of the tablet (Long and Alderton, 1960; Mazel et al.,  
50 2015). Another factor is the kinematic friction between the powder/tablet and the die.  
51 It was shown that the kinematic friction coefficient increases with the sliding speed  
52 and that this speed dependency is an intrinsic property of the friction between a  
53 tablet and a die lubricated with magnesium stearate (Desbois et al., 2019).

54 Other aspects of the SRS are directly linked with the intrinsic mechanical properties  
55 of the compressed powder. Viscoplasticity means that the plastic deformation is time-  
56 dependent and viscoelasticity means that the elastic (recoverable) deformation is  
57 time-dependent (Alderborn and Nyström, 1996; Vincent, 2012). Both aspects have  
58 been studied (Çelik and Aulton, 1996; Katz and Buckner, 2013; Malamataris and  
59 Rees, 1993; Morehead, 1992; Radebaugh et al., 1989; Rees and Rue, 1978; Rippie  
60 and Danielson, 1981; Tye et al., 2005). Unfortunately, in the literature, the different  
61 aspects of the SRS are often mixed. To precisely define the SRS, it would be of  
62 interest to define a methodology that makes it possible to separate the different  
63 aspects.

64 This work is focused on viscoelasticity. In the literature, two main approaches were  
65 used to characterize viscoelasticity. The first one consists in characterizing the tablet  
66 after ejection (i.e. "out of die"). Several articles have presented methodologies with  
67 this approach using relaxation tests or dynamic mechanical analysis (Ascani et al.,  
68 2019; Çelik and Aulton, 1996; Hancock et al., 2001; Radebaugh et al., 1989).  
69 Nevertheless, these approaches have several drawbacks. First, only products that  
70 make it possible to obtain intact tablets after ejection can be used. Then, the forces  
71 used for the characterization are generally very low and far from the loads used  
72 during compaction. Finally, the characterization is often unidirectional, meaning that

73 only one elastic modulus is characterized in terms of viscoelasticity whereas a  
74 complete description would need the use of two different moduli.

75 The second method is to observe the viscoelasticity directly in the die, before tablet  
76 ejection. Several articles were published using a relaxation test at the compression  
77 top (Casahoursat et al., 1988; Rees and Tsardaka, 1993; Rehula et al., 2012). But at  
78 the compression top, both viscoelasticity and viscoplasticity are occurring. It is thus  
79 not a true viscoelastic characterization. Another approach is the use of the unloading  
80 part of the compaction cycle, where deformation is supposed to be elastic (Rippie  
81 and Danielson, 1981). Nevertheless, in the literature, it was also shown that plastic  
82 deformation takes place during most of the unloading step (Hiestand et al., 1977).  
83 Finally, other techniques were proposed like the use of ultrasounds (Saeedi Vahdat  
84 et al., 2013).

85 In this work, we propose an original experimental methodology to characterize  
86 specifically the viscoelasticity of a tablet directly in the die. This methodology makes it  
87 possible to separate viscoelasticity from the other kinds of time-dependent  
88 deformations.

89 Beyond the characterization of viscoelasticity, another objective of this study was to  
90 model the viscoelastic behavior with the objective of integrating this behavior in  
91 numerical simulations. Currently, Finite Element Method (FEM) is mainly used for the  
92 modelling of powder compaction. The models used (e.g. Drucker Prager Cap) are  
93 essentially time independent. In order to represent the viscoelastic behavior using  
94 FEM, a mathematical formulation of the viscoelastic behavior must be found. In this  
95 work, the time evolution of elastic moduli was represented using Prony series and

96 model parameters were found by inverse identification using an analytical approach  
97 and FEM simulations.

## 98 **2. Material and method**

### 99 **2.1. Materials**

#### 100 **2.1.1. Powders**

101 Four pharmaceutical excipients were used: Lactose Monohydrate (GLac) (Excipress,  
102 ArmorPharma, Maen Roch, France), Anhydrous Calcium Phosphate (ACP) (DiCafos  
103 A60, Chemische Fabrik Budenheim, Budenheim, Germany), Microcrystalline  
104 Cellulose (MCC) (Vivapur200, JRS Pharma, Weissenborn, Germany) and Starch  
105 (Lycatab C, Roquette, Lestrem, France). Magnesium Stearate was used for external  
106 lubrication (Partek Mg Lub, Merck, Darmstadt, Germany).

#### 107 **2.1.2. Powder compaction**

108 All compaction experiments were performed on a compaction simulator Styl'One  
109 Evolution (Medelpharm, Beynost, France). This machine is instrumented with load  
110 sensors (strain gauges) and displacement sensors (incremental sensors) on each  
111 punch. The die-wall pressure is measured with an instrumented die (strain gauge).  
112 For the experiments, round flat punches with a diameter of 11.28 mm were used.

113 An external system was used to lubricate the punches and the die. This system used  
114 a pulsed air blow cabinet to spray the Magnesium Stearate powder on the punches  
115 and die. Precise compaction conditions are explained below.

#### 116 **2.1.3. Numerical simulation**

117 FEM was used for numerical modelling. All simulations were performed using the  
118 software Abaqus® (Abaqus® Standard 6.13, Dassault Systèmes, Vélizy-Villacoublay,

119 France). To represent the compaction process, the die and punches were modelled  
120 as analytical rigid surfaces and the tablet was defined as a continuous deformable  
121 solid. For symmetry reasons, axysymmetrical simulations were performed. A friction  
122 coefficient dependent of the speed was used to represent the friction between the  
123 tooling and the tablet during compression. Its value was taken from a previous  
124 publication (Desbois et al., 2019). Linear elastic and viscoelastic laws with Prony  
125 series were used.

## 126 **2.2. Theoretical background: Linear viscoelasticity**

127 In the case of linear elasticity, the relation between the strain of a solid ( $\epsilon$ ) and the  
128 applied stress ( $\sigma$ ) can be represented by Hook's law:

$$\sigma = E\epsilon \quad (1)$$

129 In the case of linear viscoelasticity, the previous equation can be replaced by an  
130 integral form (Marques and Creus, 2012):

131

$$\sigma(t) = \int_0^t E(t - \tau) \frac{d\epsilon(\tau)}{d\tau} d\tau \quad (2)$$

132 In this case, if Young's modulus depends on time, the stress-strain relationship is a  
133 function of the loading history ( $t=0$  represents the beginning of the loading history).

134 Previous equations represent the 1D case. For 3D cases, it is possible to extend this  
135 approach using the deviatoric and volumetric parts of stresses and strains (Rippie  
136 and Danielson, 1981). This implies the use of the bulk (K) and shear (G) moduli. In  
137 these cases, the evolutions of the deviatoric (q) and the hydrostatic (p) stresses are  
138 given by the following relations (Marques and Creus, 2012):

$$q(t) = \int_0^t G(t - \tau) \frac{d\varepsilon_s(\tau)}{d\tau} d\tau \quad (3)$$

139

$$p(t) = \int_0^t K(t - \tau) \frac{d\varepsilon_v(\tau)}{d\tau} d\tau \quad (4)$$

140

141 with  $\varepsilon_s$  and  $\varepsilon_v$  the deviatoric and volumetric strains respectively.

142 To use equations (3) and (4), it is necessary to propose an analytical form of the  
 143 time dependency of K and G. The most classical form is the Prony series. Prony  
 144 series are derived from the generalized Maxwell model. They can be expressed  
 145 as (Marques and Creus, 2012):

$$G(t) = G_\infty \left( 1 + \sum_{i=1}^n g_i e^{-t/\tau_i} \right) \quad (5)$$

$$K(t) = K_\infty \left( 1 + \sum_{i=1}^n k_i e^{-t/\tau_i} \right) \quad (6)$$

146

147 where  $G_\infty$  and  $K_\infty$  are the infinite shear and bulk moduli and  $g_i$ ,  $k_i$  and  $\tau_i$  are model  
 148 parameters.

149 A complete characterization of the viscoelastic behavior of a solid using this model  
 150 means the determination of all the constants included in the previous equations. This  
 151 work presents a methodology for such a characterization.

### 152 **2.3. Experimental protocol for the characterization of the viscoelasticity**



153 To characterize viscoelasticity, it is important to design experiments where the tablet  
154 is deformed only elastically. This is for example not the case for relaxation  
155 experiments performed at the compaction top. For this purpose, a specific  
156 compaction cycle was defined and is presented in figure 1.

157 A first compression was performed to make the tablet. Furthermore, an extended  
158 dwell time was used to complete as much as possible the viscoplastic effects. This  
159 first compression defines the tablet that will be studied. In this work two first pressure  
160 levels were used: 100MPa and 200 MPa. Using these two different first pressures  
161 made it possible to obtain, for each product, tablets with two different porosity  
162 levels. These two values of pressure were chosen arbitrarily but are consistent with  
163 classical pressures used to obtain tablets. Thus, for each product, two sets of data  
164 will be presented: one for the tablets obtained under 100 MPa and one for the tablets  
165 obtained under 200 MPa.

166 After this first compression (either at 100MPa or at 200MPa), two more compressions  
167 with extended dwell times were performed at a pressure lower than the first one in  
168 order to complete as much as possible the plastic and viscoplastic deformations.

169 Finally, the viscoelastic properties were measured during the fourth compaction. The  
170 displacement during this compaction was set between 50 and 100  $\mu\text{m}$  (depending on  
171 the product) which corresponds to a global strain between 1.75% and 3.5%. These  
172 values were chosen as a trade-off between a displacement value sufficiently high to  
173 ensure the precision of the measurements and overpass the initial non-linear  
174 elasticity (Brewin et al., 2007), and sufficiently low to remain in the linear viscoelastic  
175 domain. The compaction speed of this fourth step was varied in order to have loading  
176 times between 30 and 30000 ms with a nearly constant speed. Times were adjusted

177 as a function of the displacement to obtain, for each product, strain rates around 1,  
178 0.1, 0.01 and  $0.001\text{s}^{-1}$ . It must be noted that for ACP and GLac, it was not possible  
179 to obtained reliable results for the strain rate  $1\text{s}^{-1}$ . So for these products only three  
180 strain rates will be presented. Times longer than 30000ms were not used because  
181 the normal compression time is often less than a few hundred milliseconds. The  
182 results presented here will thus focus on the viscoelasticity occurring during  
183 compression and not on very long term viscoelasticity (occurring during hours or  
184 days). With the compaction simulator used, it was also impossible to obtain a reliable  
185 signal for a compaction time under 30ms, especially because the speed was not  
186 constant during loading.

187 During the loading at different strain rate (or time), the viscoelastic behavior of a  
188 tablet can be approximated by an apparent linear elastic behavior, with apparent  
189 elastic constants that change from one loading time to another (Mattei and Ahluwalia,  
190 2019). A previously published method (Mazel et al., 2012) was used to determine the  
191 apparent Young's modulus (E) and Poisson's Ratio ( $\nu$ ). Finally, apparent K and G  
192 were calculated for the different loading times using the following equations (Landau  
193 and Lifshitz, 1959):

$$K = \frac{E}{3(1 - 2\nu)} \quad (7)$$

$$G = \frac{E}{2(1 + \nu)} \quad (8)$$

194 For each condition, 5 tablets were produced.

### 195 **3. Results and discussion**

#### 196 **3.1. Experimental characterization of viscoelasticity**

197 Before applying the methodology described above, it was important to verify that no  
198 viscoelastic effect was introduced by the press itself. The compaction system has  
199 indeed an elastic compliance, i.e. it deforms elastically during loading and unloading.  
200 It was thus important to verify that this elastic deformation was not time dependent.  
201 To measure the elastic deformation of the press, a steel gage was compressed  
202 between the two punches. The deformation of the gage, even if very small, was taken  
203 into account in the measure of the press deformation (Young's modulus of steel  
204  $E=220$  GPa). For this experiment, the gage was compressed between 0 and 90 MPa,  
205 which covers the range used in the fourth compression. This was done for  
206 compression times of 30, 300, 3000 and 30000 ms. This corresponds to the range of  
207 compression times used in our protocol for viscoelasticity determination. Results are  
208 presented in figure 2. The different runs are perfectly superimposed which means  
209 that no viscoelastic effect is introduced by the press itself. The elastic compliance of  
210 the press was taken into account in the measurement of the displacements.

211 The original in die method described above was then applied to four excipients to  
212 determine their viscoelastic behavior. The final porosities of the tablets obtained for  
213 each product and each pressure point are presented in table 1. No significant  
214 differences were found between tablets made with the same product and the same  
215 first pressure but with different loading time for the last compression. As a  
216 consequence, only one value of porosity for each first compression pressure is  
217 reported in table 1.

218 The apparent elastic moduli measured during the experiments are presented in table  
219 2 and figures 3 and 4. For MCC and Starch, results in table 2 indicate that both K and  
220 G are dependent on the strain rate. More precisely, K and G increase when the strain  
221 rate increases, which is expected in the case of a viscoelastic product. To better

222 illustrate the variations, values of K and G normalized by the value obtained for the  
223 smallest strain rate (longest loading time) are presented in figures 3 and 4. For  
224 starch, at a strain rate of  $0.1\text{s}^{-1}$ , the increase was between 32% and 38% for G and  
225 between 21% and 24% for K. For MCC we obtained, for the same strain rate an  
226 increase of G and K between 14% and 20%, and 4% and 12% respectively. On the  
227 contrary, changes observed for ACP and GLac were always below 5% whatever the  
228 strain rate.

229 The excipients used in this study were chosen based on their mechanical behaviors  
230 as described in the literature. Starch is known to be a viscoelastic product and MCC  
231 present also some viscoelasticity (Malamataris and Rees, 1993; Van der Voort  
232 Maarschalk et al., 1997). On the contrary, ACP and GLac are not expected to show  
233 significant viscoelasticity. The results presented above are thus totally coherent with  
234 the existing literature: starch is the most viscoelastic of the four products and MCC  
235 also presents some viscoelasticity. On the contrary, the viscoelasticity of GLac and  
236 ACP is very low as expected. These results make it thus possible to validate the  
237 present methodology for the determination of the viscoelastic properties of  
238 pharmaceutical tablets. Based on these results, GLac and ACP show very limited  
239 viscoelasticity even if the strain rate range was three decades. Viscoelasticity can  
240 thus be neglected, on the time range studied in this work, in the mechanical behavior  
241 of these two products. The following parts of the article will thus focus on the results  
242 obtained on MCC and starch.

243 Besides showing that MCC and starch are indeed viscoelastic products, the  
244 methodology developed makes it possible to study both the volumetric and the  
245 deviatoric part of viscoelasticity. Generally, in the literature, the volumetric part of  
246 viscoelasticity is neglected compared to the deviatoric part. This was for example

247 done in the studies performed in the pharmaceutical field on the unloading part of the  
248 compaction profile (Rippie and Danielson, 1981). Such a hypothesis would mean that  
249 K should remain constant and that only G should vary with the strain rate. Results  
250 presented in figures 3 and 4 clearly show that the volumetric part of the viscoelasticity  
251 cannot be neglected in the case pharmaceutical tablets. Even if G shows greater  
252 variations than K, K is also varying with the strain rate.

253 As explained above, the purpose of using two different first compression pressures  
254 (100 MPa and 200 MPa) was to analyze the viscoelasticity with two different tablets  
255 for the same product. The results of the experiments reported in table 2 show  
256 differences between both compression pressures. As expected, for all the products  
257 and for each loading time, K and G increase when the first compression pressure  
258 increase, i.e, when the porosity decreases. This was expected according to the  
259 literature (Mazel et al., 2013; Roberts et al., 1994). In figures 3 and 4, a different  
260 evolution of the viscoelasticity of each product is found when the first pressure varies.  
261 When the first compression pressure increases (i.e. reduced porosity, see table 1),  
262 normalized G and K increase for Starch, however, for MCC the normalized moduli  
263 decrease. These results imply two different behaviors. For Starch the viscoelasticity  
264 increases and for MCC the viscoelasticity decreases when the porosity decreases.  
265 These results are very preliminary, and a complete understanding of this phenomena  
266 would require further work that overpasses the objectives of this study.

267 Finally, the proposed characterization method made it possible to characterize the  
268 viscoelasticity of the different products qualitatively and quantitatively. For each  
269 product, we obtained a couple of K and G associated with a loading time. The  
270 following objective of this work was to find a model that represents correctly this  
271 viscoelastic behavior and that could be introduced in FEM simulation.

## 272 3.2. Modeling of the viscoelastic behavior

273 As explained above, to be able to use equations (3) and (4) to represent the  
274 viscoelastic behavior of the powders, it is necessary to choose an analytical  
275 expression of K and G. As often done, Prony series were chosen in this study for this  
276 purpose. The objective of this part is to determine the coefficients of the Prony series  
277 for G and K that make it possible to represent the viscoelastic behavior found in the  
278 previous experiments for Starch and MCC. The first step was to find approximate  
279 coefficients of the Prony series with an analytic approach. In a second step, using  
280 FEM simulation, friction between the die and the tablet was taken into account.

### 281 3.2.1. Analytical development of the Prony series

282 In our experiments, the loading speed is constant, which implies that the strain rate is  
283 also approximately constant:

$$\frac{d\varepsilon(\tau)}{d\tau} = \frac{\varepsilon}{t} = A \quad (9)$$

284 with A the strain rate ( $s^{-1}$ ).

285 In this case, the integrals from equations 3 and 4 can be easily calculated. The  
286 results for the evolution of q and p as a function of time can be found in the following  
287 equations:

$$q(t) = AG_{\infty} \left[ t + \sum_{i=1}^n g_i e^{-t/\tau_i} \times \tau_i (e^{t/\tau_i} - 1) \right] \quad (10)$$

$$p(t) = AK_{\infty} \left[ t + \sum_{i=1}^n k_i e^{-t/\tau_i} \times \tau_i (e^{t/\tau_i} - 1) \right] \quad (11)$$

288 Using equations (10) and (11), it is possible to calculate the apparent K and G for the  
289 different loading times. The apparent moduli found are function of the parameters of  
290 the prony series. The aim was then to find the parameters of the prony series that  
291 make it possible to obtain analytically apparent moduli close to those found  
292 experimentally.

293 The first step was to decide how many terms to use in the prony series. It is common  
294 to consider one characteristic time ( $\tau_i$ ) per decade. Considering the analytical  
295 protocol developed, we chose to use three characteristic times: 30 ms, 300ms and  
296 3000ms. We thus used Prony series with three terms.

297 The experiments at 30000 ms were considered as quasi-static and were used as a  
298 first approximation for  $K_\infty$  and  $G_\infty$ . Finally, to determine the different  $g_i$  and  $k_i$ , a  
299 reverse identification with the experiments was performed.  $g_i$  and  $k_i$  values were  
300 adjusted manually until the apparent moduli calculated matched the experimental  
301 values.

302 Comparison between the experimental and calculated values at the end of the  
303 adjustment process can be found in table 3. As it can be seen, the Prony series make  
304 it possible to represent the viscoelastic evolution obtained experimentally with a great  
305 precision (errors are always lower than 1%). This shows that the analytical approach  
306 proposed gives very good results. Nevertheless, it contains simplifications compared  
307 to the performed experiments. Indeed, it considers that the whole tablet is submitted  
308 to homogeneous stresses, which is not strictly correct because of the friction between  
309 the tablet and the die. Moreover, friction between the tablet and the die was found  
310 previously to depend on the speed of compaction (Desbois et al., 2019). In order to  
311 take into account these effects, the finite element method was finally used.

### 312        **3.2.2. Finite element method integration**

313    As mentioned previously, all the simulations were performed using the software  
314    Abaqus®. Viscoelasticity based on prony series is already implemented in the code.  
315    Nevertheless, in Abaqus®, Prony series formulation is slightly different from the  
316    expression presented above. In equation 5 and 6,  $g_i$  and  $k_i$  correspond to moduli  
317    normalized with respect to the infinite moduli ( $G_\infty, K_\infty$ ). In Abaqus, the parameters  
318    correspond to moduli normalized with respect to the initial moduli. The parameters  
319    calculated above had thus to be transformed in order to be implanted in the code.  
320    Nevertheless, for clarity reasons, in the following text, we will still express the  
321    parameters of the Prony series based on infinite moduli as formulated in equation 5  
322    and 6.

323    The simulations carried out represent compressions with the experimental loading  
324    times (30ms, 300ms, 3000ms). The simulation generates the evolution of the axial  
325    and radial forces and the thickness of the tablet. These values were used to calculate  
326    the stresses and strains on the tablet during the loading and thus to determine the  
327    apparent elastic moduli as explained above.

328    The simulations were first performed with the parameters determined analytically,  
329    then parameters were varied to find apparent moduli as close as possible to the  
330    experimental values. The calculations were applied to the two viscoelastic products  
331    studied before, MCC and starch.

332    The only difference between the analytical approach and the FEM approach is the  
333    introduction of friction. The results obtained in the simulation showed that friction only  
334    promotes a slight increase of all the apparent moduli of a nearly constant value. As a  
335    consequence, to improve the correspondence between simulated and experimental



336 values it was only found necessary to lower slightly (around 0.5%) the infinite moduli  
337 without changing the  $g_i$  and  $k_i$  parameters. The values obtained were very similar to  
338 those presented in table 3 with an error between the experimental and the numerical  
339 values always lower than 1%. This means that Prony series are well suited to  
340 represent the viscoelastic behavior of pharmaceutical tablet during FEM modelling.

341 Table 4 shows the coefficients of the Prony series used in the simulations for MCC  
342 and Starch. The  $g_i$  and  $k_i$  show the same trend as those found in Figure 3 and Figure  
343 4. For example, the  $g_i$  are higher than the  $k_i$  which means that the deviatoric behavior  
344 is more important than the volumetric behavior. Nevertheless, the parameters make it  
345 possible to go a little bit further in the characterization of the viscoelastic behavior  
346 because they give access to the importance of the different characteristic times. It is  
347 interesting to note that viscoelasticity is present at both long and short characteristic  
348 times. Viscoelasticity at long characteristics times was expected. It is indeed well-  
349 known that tablets of starch or MCC keep expanding after ejection and that this  
350 expansion continues during several hours. The term at 3000 ms could correspond to  
351 an expansion just after unloading. Of course, it is possible that longer times might  
352 also be present but they overpass the objectives of this study which is more focused  
353 on the characteristic times occurring during compression.

354 The results presented in table 4 also show that viscoelasticity is not limited to long  
355 times. The term at 30ms is important in all the cases. Especially, in the deviatoric  
356 part, this term is always the largest. The short time terms are those which are the  
357 most important during compaction (the compaction cycle is generally much less than  
358 1s). This means that viscoelasticity indeed plays a role during compaction. Thus,  
359 including it for example in numerical modelling is mandatory to correctly represent the  
360 compaction behavior of certain kind of products.

#### 361 **4. Conclusion**

362 Strain rate sensitivity during tablet manufacturing is a complex phenomenon. It is  
363 composed of different phenomena like air entrapment, kinematic friction,  
364 viscoplasticity or viscoelasticity. The methodology developed in this work made it  
365 possible to isolate the viscoelasticity of the material with a special compression cycle  
366 using different strain rates. Four different pharmaceutical excipients were studied with  
367 success and it was found, as expected, that GLac and ACP have very limited  
368 viscoelasticity, contrary to MCC and starch. Moreover, Starch was found more  
369 viscoelastic than MCC.

370 Prony series were used to represent analytically the viscoelastic behavior. Prony  
371 series terms were first identified using an analytical approach. Then a FEM numerical  
372 approach was used to refine the results by taking friction into account. It was found  
373 that Prony series made it possible to correctly represent the viscoelastic behavior of  
374 pharmaceutical tablets. Moreover, the Prony series parameters obtained made it  
375 possible to quantify the viscoelastic behavior.

376 In addition to a new methodology to quantify viscoelasticity, the present study  
377 highlights two important results. First, in the case of pharmaceutical tablets,  
378 viscoelasticity is not limited to deviatoric terms. The volumetric part, even if less  
379 important, cannot be neglected, contrary to what was supposed in the  
380 pharmaceutical literature. The other point is that viscoelasticity is present at short and  
381 long times. The short time terms indicate that viscoelasticity might play a role during  
382 compaction and not only during post compaction relaxation. It must be noted that  
383 shorter times effects might also be present but that it was not possible to characterize  
384 them with the present methodology.

385 As shown in this article, the apparent elastic moduli of a pharmaceutical tablet might  
386 be influenced by the strain rate. This is important to consider when comparing results  
387 of elastic moduli found in different studies as tableting conditions might differ greatly  
388 from one study to the other.

389 Finally, Prony series could be used in numerical simulation to represent the  
390 viscoelastic behavior of a powder during compression. Nevertheless, some code  
391 limitation may arise. For example, in the current version of Abaqus<sup>®</sup> (6.13), it is not  
392 possible to use simultaneously viscoelasticity and plasticity. The use of this model  
393 might thus require the development of user defined mechanical behavior in FEM  
394 codes.

### 395 **Acknowledgement**

396 The authors acknowledge the support of the French Agence Nationale de la  
397 Recherche (ANR), under grant ANR-17-CE08-0015 (project CliCoPha).

### 398 **Legend to figures**

399 Figure 1: Typical evolution of the compaction pressure vs time for the proposed  
400 protocol: a) Example of evolution during the whole compaction cycle; b) Examples of  
401 4<sup>th</sup> compactions at different strain rates.

402 Figure 2: Total press deformation as a function of the axial pressure for different  
403 compression times.

404 Figure 3: Normalized shear modulus as a function of the strain rate.

405 Figure 4: Normalized bulk modulus as a function of the strain rate.

### 406 **References**

407 Alderborn, G., Nyström, C., 1996. Pharmaceutical powder compaction technology.  
408 Marcel Dekker, New York.

409 Armstrong, N.A., 1989. Time-dependent factors involved in powder compression and  
410 tablet manufacture. *International Journal of Pharmaceutics* 49, 1–13.

411 Ascani, S., Berardi, A., Bisharat, L., Bonacucina, G., Cespi, M., Palmieri, G.F., 2019.  
412 The influence of core tablets rheology on the mechanical properties of press-  
413 coated tablets. *European Journal of Pharmaceutical Sciences* 135, 68–76.  
414 <https://doi.org/10.1016/j.ejps.2019.05.011>

415 Brewin, P.R., Coube, O., Doremus, P., Tweed, J.H., 2007. *Modelling of Powder Die*  
416 *Compaction*. Springer Science & Business Media.

417 Casahoursat, L., Lemagnen, G., Larrouture, D., 1988. The Use of Stress Relaxation  
418 Trials to Characterize Tablet Capping. *Drug Development and Industrial*  
419 *Pharmacy* 14, 2179–2199.

420 Çelik, M., Aulton, M.E., 1996. The Viscoelastic Deformation of Some Tableting  
421 Materials as Assessed by Indentation Rheology. *Drug Development and*  
422 *Industrial Pharmacy* 22, 67–75.

423 Desbois, L., Tchoreloff, P., Mazel, V., 2019. Influence of the Punch Speed on the Die  
424 Wall/Powder Kinematic Friction During Tableting. *JPharmSci* 108, 3359–3365.

425 Garr, J.S.M., Rubinstein, M.H., 1991. An investigation into the capping of  
426 paracetamol at increasing speeds of compression. *International Journal of*  
427 *Pharmaceutics* 72, 117–122.

428 Hancock, B.C., Dalton, C.R., Clas, S.-D., 2001. Micro-scale measurement of the  
429 mechanical properties of compressed pharmaceutical powders. 2: The  
430 dynamic moduli of microcrystalline cellulose. *International Journal of*  
431 *Pharmaceutics* 228, 139–145.

432 Hiestand, E.N., Wells, J.E., Peot, C.B., Ochs, J.F., 1977. Physical processes of  
433 tableting. *J. Pharm. Sci.* 66, 510–519.

434 Katz, J.M., Buckner, I.S., 2013. Characterization of strain rate sensitivity in  
435 pharmaceutical materials using indentation creep analysis. *International*  
436 *Journal of Pharmaceutics, Manufacturing Performance of Solid Dosage Forms*  
437 442, 13–19.

438 Landau, L.D., Lifshitz, E.M., 1959. *Theory of Elasticity, Course of theoretical physics.*  
439 Pergamon Press, London.

440 Long, W.M., Alderton, J.R., 1960. The displacement of gas from powders during  
441 compaction. *Powder Metallurgy* 3, 52–72.

442 Malamataris, S., Rees, J.E., 1993. Viscoelastic properties of some pharmaceutical  
443 powders compared using creep compliance, extended Heckel analysis and  
444 tablet strength measurements. *International Journal of Pharmaceutics* 92,  
445 123–135.

446 Marques, S.P.C., Creus, G.J., 2012. *Computational Viscoelasticity*. Springer, Berlin  
447 Heidelberg.

448 Mattei, G., Ahluwalia, A., 2019. A new analytical method for estimating lumped  
449 parameter constants of linear viscoelastic models from strain rate tests. *Mech*  
450 *Time-Depend Mater* 23, 327–335.

451 Mazel, V., Busignies, V., Diarra, H., Tchoreloff, P., 2015. Lamination of  
452 pharmaceutical tablets due to air entrapment: Direct visualization and  
453 influence of the compact thickness. *International Journal of Pharmaceutics*  
454 478, 702–704.

455 Mazel, V., Busignies, V., Diarra, H., Tchoreloff, P., 2013. On the Links Between  
456 Elastic Constants and Effective Elastic Behavior of Pharmaceutical Compacts:

457 Importance of Poisson's Ratio and Use of Bulk Modulus. *Journal of*  
458 *Pharmaceutical Sciences* 102, 4009–4014.

459 Mazel, V., Busignies, V., Diarra, H., Tchoreloff, P., 2012. Measurements of elastic  
460 moduli of pharmaceutical compacts: A new methodology using double  
461 compaction on a compaction simulator. *J. Pharm. Sc.*

462 Morehead, W.T., 1992. Viscoelastic Behavior of Pharmaceutical Materials During  
463 Compaction. *Drug Development and Industrial Pharmacy* 18, 659–675.

464 Radebaugh, G.W., Babu, S.R., Bondi, J.N., 1989. Characterization of the viscoelastic  
465 properties of compacted pharmaceutical powders by a novel nondestructive  
466 technique. *International Journal of Pharmaceutics* 57, 95–105.

467 Rees, J.E., Rue, P.J., 1978. Time-Dependent Deformation of Some Direct  
468 Compression Excipients. *Journal of Pharmacy and Pharmacology* 30, 601–  
469 607.

470 Rees, J.E., Tsardaka, K.D., 1993. Compaction stress relaxation interpreted using a  
471 hyperbolic relation. *International Journal of Pharmaceutics* 92, 137–141.

472 Rehula, M., Adamek, R., Spacek, V., 2012. Stress relaxation study of fillers for  
473 directly compressed tablets. *Powder Technology* 217, 510–515.  
474 <https://doi.org/10.1016/j.powtec.2011.11.011>

475 Rippie, E.G., Danielson, D.W., 1981. Viscoelastic stress/strain behavior of  
476 pharmaceutical tablets: Analysis during unloading and postcompression  
477 periods. *J. Pharm. Sci.* 70, 476–482.

478 Roberts, R.J., Rowe, R.C., York, P., 1994. The Poisson Ratio of Microcrystalline  
479 Cellulose. *International Journal of Pharmaceutics* 105, 177–180.

480 Saeedi Vahdat, A., Krishna Prasad Vallabh, C., Hancock, B.C., Cetinkaya, C., 2013.  
481 Ultrasonic approach for viscoelastic and microstructure characterization of  
482 granular pharmaceutical tablets. *International Journal of Pharmaceutics, A*  
483 *Position Paper and Commentaries on More effective advanced drug delivery*  
484 *systems* 454, 333–343. <https://doi.org/10.1016/j.ijpharm.2013.06.045>

485 Tye, C.K., Sun, C. (Calvin), Amidon, G.E., 2005. Evaluation of the effects of tableting  
486 speed on the relationships between compaction pressure, tablet tensile  
487 strength, and tablet solid fraction. *Journal of Pharmaceutical Sciences* 94,  
488 465–472. <https://doi.org/10.1002/jps.20262>

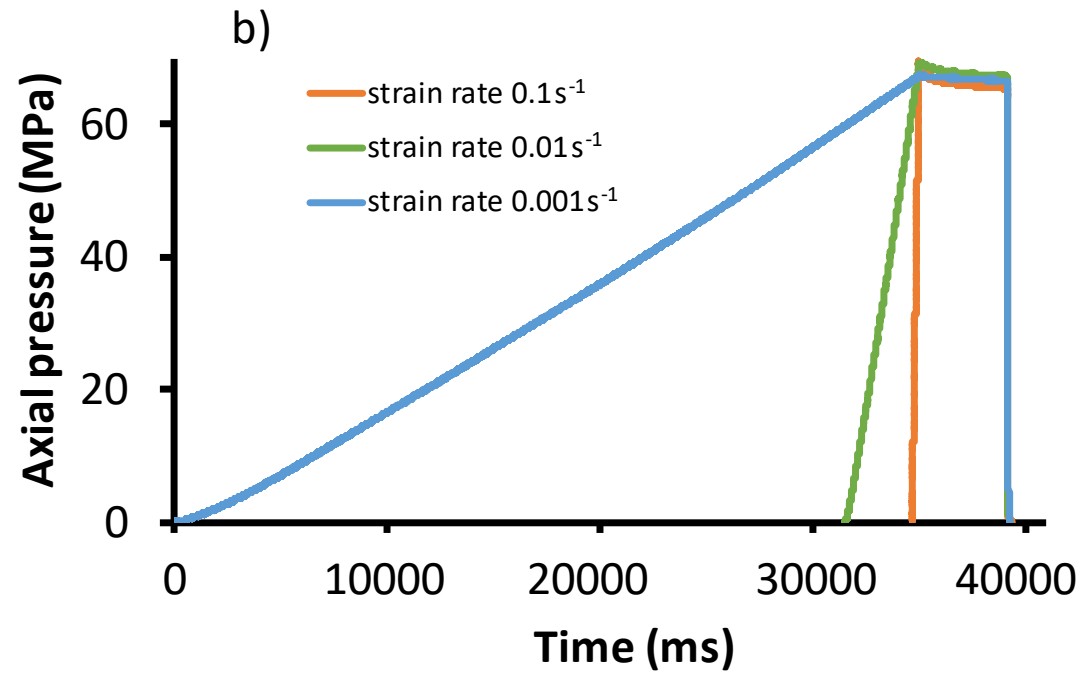
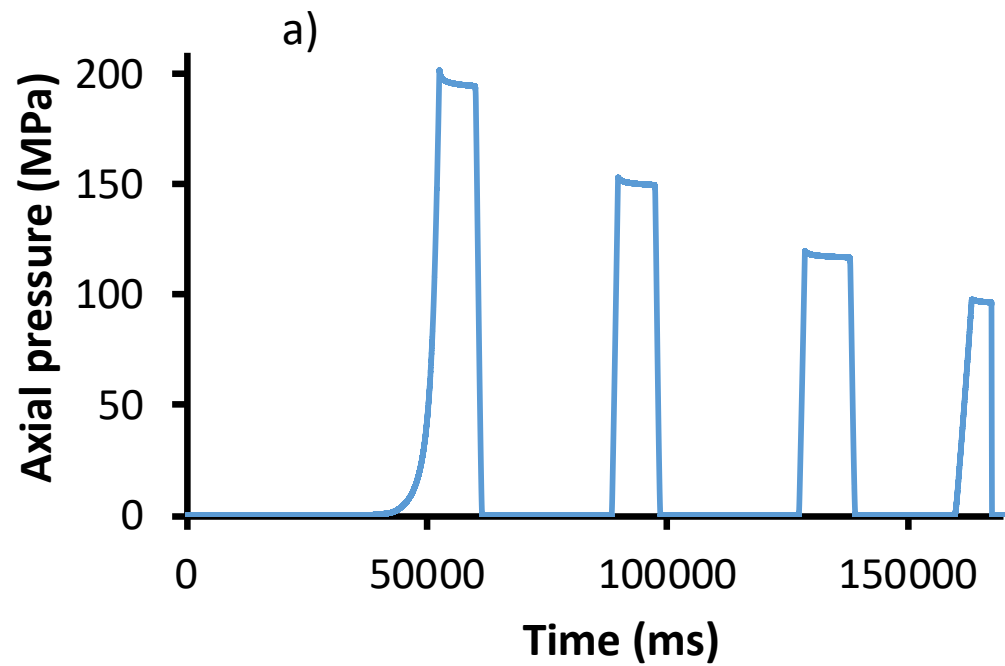
489 Van der Voort Maarschalk, K., Zuurman, K., Vromans, H., Bolhuis, G.K., Lerk, C.F.,  
490 1997. Stress relaxation of compacts produced from viscoelastic materials.  
491 *International Journal of Pharmaceutics* 151, 27–34.

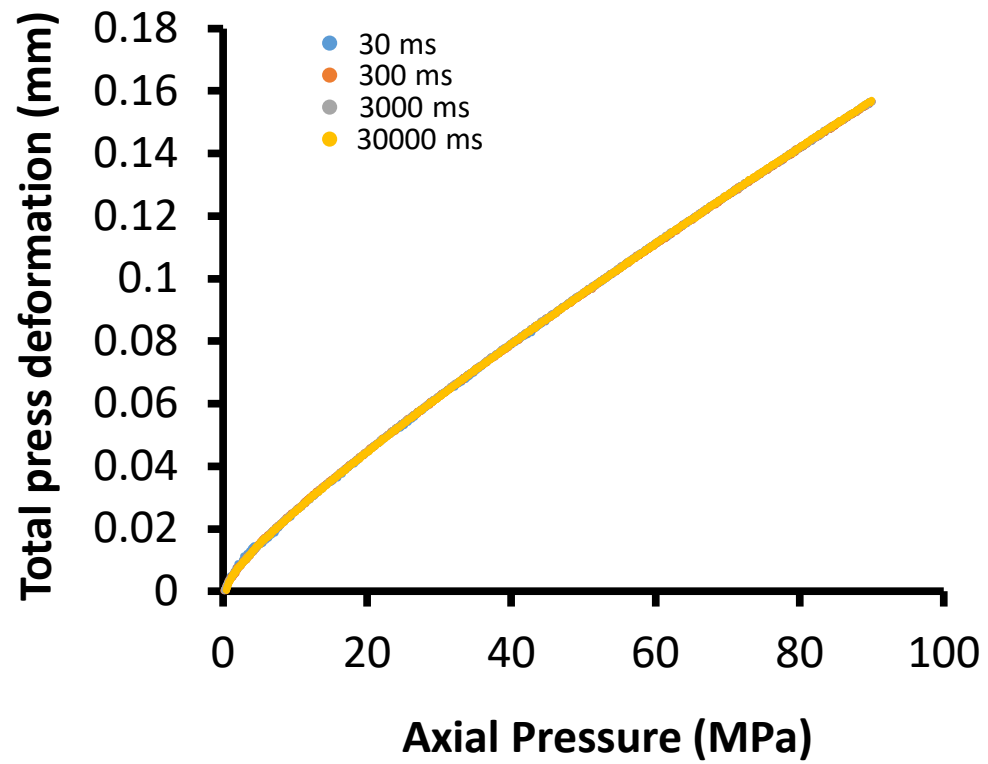
492 Vincent, J., 2012. *Structural Biomaterials*, Third edition. ed. Princeton University  
493 Press, Princeton.

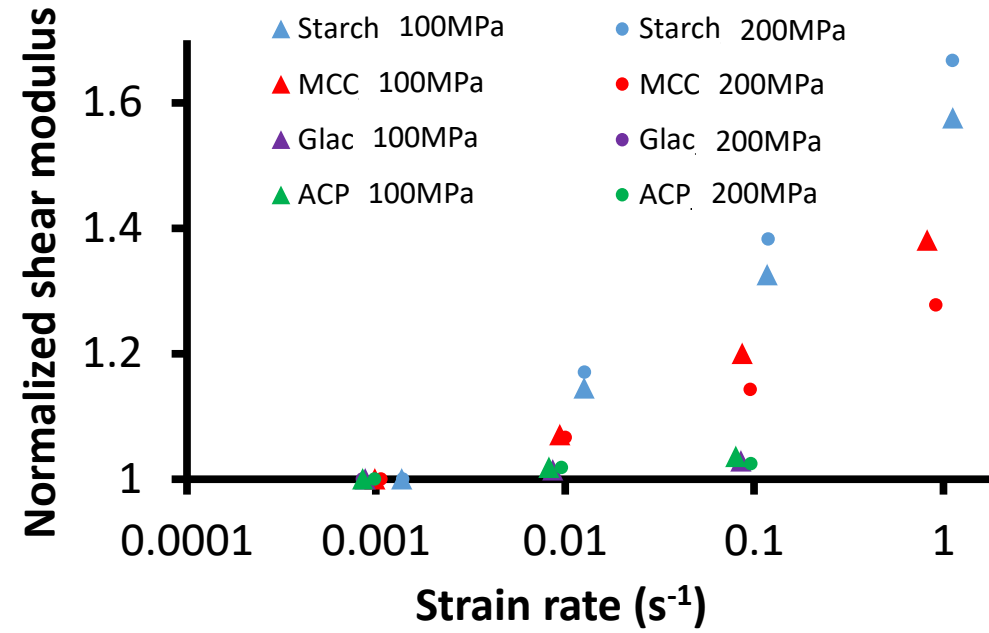
494

495

496









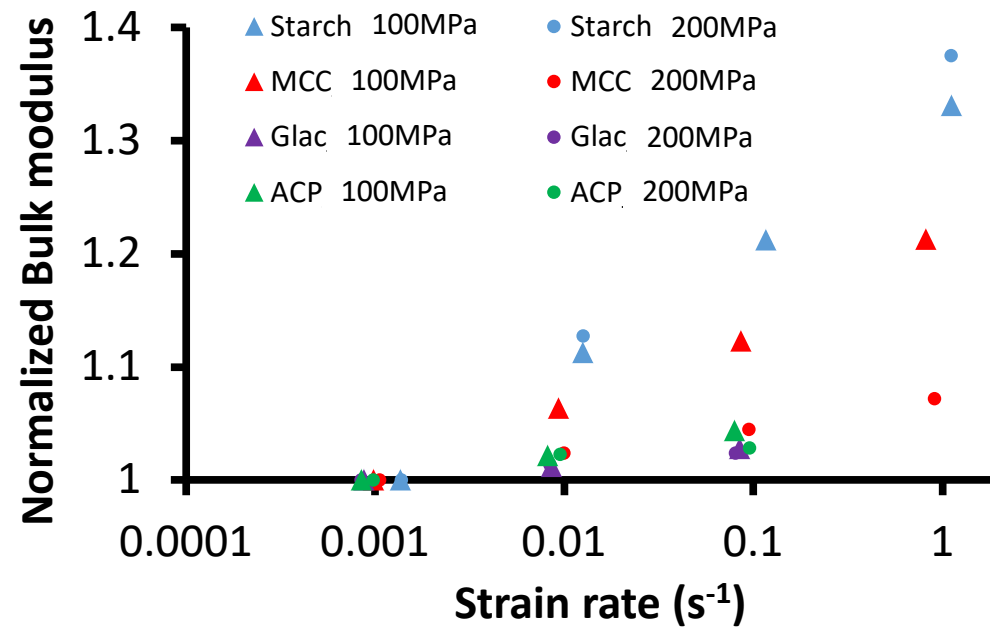


Table 1: Porosity of the tablets obtained after ejection. True density was determined using Helium pycnometry (Accupyc 1340, Micromeretics, Norcross, USA).

Product	True density (g.cm <sup>-3</sup> )	First compression pressure (MPa)	Porosity(%)
ACP	2.857	100	32.4 ± 0.1
		200	26.2 ± 0.1
Glac	1.549	100	16.2 ± 0.1
		200	10.2 ± 0.1
MCC	1.566	100	12.3 ± 0.2
		200	5.9 ± 0.3
Starch	1.485	100	10.5 ± 0.3
		200	6.4 ± 0.1

Table 2: Apparent elastic constants obtained for all the products (standard deviation between parentheses)

Apparent elastic moduli		E (MPa)		$\nu$		G(MPa)		K(MPa)	
First compression pressure (MPa)		100	200	100	200	100	200	100	200
Product	Loading time (ms)								
MCC	30000	1428 (19.4)	2005 (11.7)	0.323 (0.002)	0.357 (0.001)	540 (7.6)	739 (5.0)	1344 (18.5)	2331 (6.5)
	3000	1529 (19.1)	2130 (16.3)	0.322 (0.002)	0.351 (0.002)	578 (7.6)	788 (6.9)	1429 (16.6)	2386 (8.8)
	300	1700 (27.5)	2273 (25.5)	0.312 (0.002)	0.344 (0.002)	648 (11.2)	845 (10.5)	1508 (14.9)	2436 (4.5)
	30	1941 (27.3)	2517 (25.6)	0.301 (0.002)	0.332 (0.002)	746 (11.2)	945 (11.1)	1629 (15.8)	2498 (13.9)
Starch	30000	634 (2.8)	681 (3.6)	0.337 (0.001)	0.344 (0.001)	237 (1.1)	253 (1.5)	649 (3.1)	729 (1.5)
	3000	723 (4.2)	795 (2.1)	0.333 (0.001)	0.339 (0.001)	271 (1.7)	297 (0.9)	722 (3.3)	822 (0.8)
	300	832 (10.2)	931 (4.7)	0.324 (0.001)	0.329 (0.001)	314 (4.1)	350 (1.9)	787 (5.0)	906 (2.5)
	30	979 (6.3)	1111 (7.4)	0.311 (0.004)	0.315 (0.001)	373 (3.2)	423 (3.1)	864 (15.6)	1003 (5.1)
ACP	20000	7336 (51.1)	9755 (36.4)	0.191 (0.001)	0.195 (0.001)	3079 (22.3)	4082 (17.2)	3959 (24.4)	5330 (19.3)
	2000	7480 (9.0)	9947 (35.2)	0.192 (0.001)	0.196 (0.001)	3138 (4.8)	4159 (18.6)	4043 (10.7)	5450 (7.7)
	200	7613 (12.1)	10005 (76.1)	0.193 (0.001)	0.196 (0.001)	3191 (6.3)	4184 (34.2)	4131 (8.2)	5481 (32.9)
Glac	17000	4380 (42.3)	5221 (24.2)	0.244 (0.001)	0.267 (0.001)	1760 (17.3)	2060 (10.2)	2857 (25.8)	3738 (14.5)
	1700	4441 (16.1)	5282 (10.7)	0.244 (0.001)	0.268 (0.001)	1785 (6.9)	2083 (5.0)	2890 (10.4)	3789 (11.7)
	170	4505 (13.2)	5374 (14.2)	0.244 (0.001)	0.266 (0.001)	1810 (6.2)	2123 (6.0)	2936 (6.1)	3827 (7.5)

Table 3: Comparison of the moduli G and K between the experiments and the analytical approach for MCC and Starch

Product	First compression pressure (MPa)	Strain rate (s <sup>-1</sup> )	G (MPa)		K (MPa)	
			Experiment	Analytic	Experiment	Analytic
MCC	100	1.000	746	747	1629	1632
		0.100	648	649	1508	1511
		0.010	578	580	1429	1431
		0.001	540	541	1344	1346
	200	1.000	945	946	2498	2502
		0.100	845	847	2436	2440
		0.010	788	790	2386	2390
		0.001	739	741	2331	2335
Starch	100	1.000	373	374	864	865
		0.100	314	315	787	788
		0.010	271	272	722	724
		0.001	237	237	649	650
	200	1.000	423	423	1003	1005
		0.100	350	351	906	907
		0.010	297	297	823	824
		0.001	253	254	730	731

Table 4: Parameters of the Prony series for MCC and Starch

Product	First comp load (MPa)	$G_i$	$K_i$	$T_i$	$E_\infty$ (MPa)	$\nu_\infty$
MCC	100	0.2330	0.1345	30	1400.8	0.323
		0.1390	0.0290	300		
		0.1130	0.1090	3000		
	200	0.1990	0.0377	30	1978.7	0.358
		0.0540	0.0107	300		
		0.1120	0.0405	3000		
Starch	100	0.3410	0.1685	30	619.7	0.338
		0.1490	0.0480	300		
		0.2430	0.1950	3000		
	200	0.3860	0.1880	30	664.7	0.346
		0.1780	0.0590	300		
		0.2880	0.2200	3000		

